ELSEVIER

Polymer 43 (2002) 5281–5288

polymer

www.elsevier.com/locate/polymer

Ionic conductivity enhancement of the plasticized PMMA/$LiClO_4$ polymer nanocomposite electrolyte containing clay

Hsien-Wei Chen, Tzu-Pin Lin, Feng-Chih Chang*

Institute of Applied Chemistry, National Chiao-Tung University, Hsin-Chu 30043, Taiwan, ROC

Received 25 February 2002; received in revised form 24 May 2002; accepted 27 May 2002

Abstract

This work has demonstrated that the addition of an optimum content of dimethyldioctadecylammonium chloride (DDAC)-modified montmorillonite clay (Dclay) enhances the ionic conductivity of the plasticized poly(methyl methacrylate)-based electrolyte by nearly 40 times higher than the plain system. Specific interactions among silicate layer, carbonyl group (C=O) and lithium cation have been investigated using Fourier-transform infrared (FTIR), solid-state NMR, alternating current impedance. The FTIR characterization confirms that both of the relative fractions of 'complexed' C=O sites and 'free' anions increase with the increase of the Dclay content, indicating that strong interaction exists between the C=O group and the lithium salt. In addition, the solid-state NMR demonstrates that the interaction between the PMMA and the clay mineral is insignificant. The addition of clay mineral promotes the dissociation of the lithium salt and thus, the specific interaction can be enhanced between the C=O and the free lithium cation. However, the balanced attractive forces among silicate layers, C=O groups, lithium cations and anions is critical to result in the higher ionic conductivity.

Keywords: Polymeric electrolytes; Ionic conductivity; Nanocomposite

1. Introduction

The interaction behavior of an alkaline ion within the polymer electrolyte would determine its applicability in high-energy density batteries and other solid-state electrochemical devices [1–4]. For most potential applications, it is desirable that the solid polymer electrolytes display a reasonable conductivity ($\sim 10^{-4}$ S cm^{-1}), dimensional stability, processability and flexibility in ambient condition. Hence, the lithium salt-based electrolytes have been the focus of a wide variety of fundamental and application-oriented studies [5,6]. However, most Li^+-based polymer electrolytes exhibit several disadvantages that limit their commercial applications. One major drawback is the relative low ionic conductivity of most electrolytes at ambient temperatures [7,8]. Various methods have been applied to increase the ionic conductivity of the electrolyte. One of the most successful approaches relies on the addition of a plasticizer to the polymer matrix forming a gel polymer electrolyte [9–12]. The gel polymer electrolyte systems based on poly(methyl methacrylate) (PMMA) [13–17] have been proposed for lithium battery application particularly because of their beneficial effects on the stabilization of the lithium–electrolyte interface [18]. However, a reasonable conductivity achieved of such plasticized film is offset by poor mechanical properties at a high concentration of the plasticizer. Rajendran et al. [13,14] reported that the blend of PMMA with poly(vinyl chloride) (PVC) is able to improve mechanical property due to its poor solubility in the plasticizer medium. However, the ionic conductivity will decrease by blending with the PVC due to the higher viscosity and lower dissociability of the lithium salt. Clay mineral is an inorganic filler with intercalation property. Intercalating polymer in the layered clay host can produce polymer nanocomposite electrolyte with huge interfacial area. From our prior studies [19,20], a higher interfacial area not only sustains the mechanical properties of PMMA-based gel polymer electrolyte but also increases the dissolubility of the lithium salts due to its higher dielectric property.

In this article, we prepared the gel polymer nanocomposite electrolyte based on PMMA, clay mineral, ethylene carbonate (EC), and $LiClO_4$ that possesses high ionic conductivity ($\sim 10^{-3}$ S cm^{-1}) and still maintains its dimensional stability.

* Corresponding author. Tel.: +886-3-5131512; fax: +886-3-5723764.
E-mail address: changfc@cc.nctu.edu.tw (F.C. Chang).

0032-3861/01/$ - see front matter
PII: S0032-3861(02)00339-7

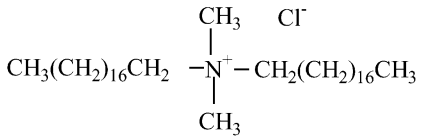

DDAC

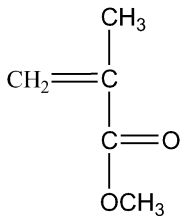

MMA

Fig. 1. The chemical structure of DDAC and MMA.

2. Experimental

2.1. Sample preparation of PMMA/clay

The methyl methacrylate (MMA) monomer and dimethyldioctadecylammonium chloride (DDAC) (Fig. 1) are both purchased from the Aldrich. The Na^+-montmorillonite (Na^+-MMT) was obtained from the Kunimine Industries Institute of Japan. These materials were used as received without any purification. The PMMA/Na^+-montmorillonite nanocomposite was prepared by two stages. In the first stage, the Na^+-MMT was organically modified by the DDAC [21]. The clay (Na^+-montmorillonite) (1 g) and 50 ml distilled water were placed in a 100 ml beaker, 1 g of DDAC was added to the solution. The mixture was stirred vigorously for 8 h, filtered and washed three times with 100 ml of hot water to remove NaCl. After being washed with ethanol (50 ml) to remove any excess of ammonium salt, the product was dried in a vacuum oven at 60 °C for 24 h. In the second stage, the specific amount of MMA monomer and DDAC-modified MMT were mixed in the toluene at 40 °C until the solution was homogeneous and then the α-α′-azobisisobutyronitrile (AIBN) initiator was added at 60 °C for about 4 h. Finally, this nanocomposite was extracted by the cyclohexane, filtered and dried in a vacuum oven at 100 °C for 24 h to remove residual solvent. The M_w of the PMMA is 15 000–20 000 by GPC measurement.

2.2. Preparation of solid polymer electrolyte

Dissolving desired amounts of the previously synthesized PMMA/clay, vacuum dried $LiClO_4$ salt and EC in the dry acetonitrile to produce PMMA/$LiClO_4$/clay/EC nanocomposites of various compositions. Following continuous stirring for 24 h at 80 °C, these solutions were maintained at 50 °C for an additional 24 h to remove the solvent, and then further dried under vacuum at 80 °C for an additional 3 days. To prevent contact with air and moisture, all nanocomposites prepared were stored in a dry box filled with nitrogen.

2.3. X-ray measurements

Wide-angle diffraction experiments were conducted on a Rigaku X-ray Diffractometer using the Cu Kα radiation (18 kW rotating anode, $\lambda = 1.5405$ Å) at 50 kV and 250 mA with a scanning rate of 2°/min.

2.4. FTIR measurements

The conventional NaCl disk method was employed to measure infrared spectra of composite films. All polymer films were prepared within an N_2 atmosphere. The acetonitrile solution was cast onto a NaCl disk from which the solvent was removed under vacuum at 70 °C for 48 h. All infrared spectra were obtained in the range from 4000 to 600 cm^{-1} using a Nicolet AVATRR 320 FTIR Spectrometer with a 1 cm^{-1} on resolution at 120 °C.

2.5. Solid-state NMR

High-resolution solid-state NMR experiments were carried out on a Bruker DSX-400 spectrometer operating at a resonance frequency of 100.47 MHz for ^{13}C. The ^{13}C CP/MAS spectra were measured with a 3.9 μs 90° pulse, with 3 s pulse delay time, 30 ms of acquisition time, and 2048 scans were accumulated. All NMR spectra were taken at 300 K using broad band proton decoupling and a normal cross-polarization pulse sequence. A magic angle sample-spinning (MAS) rate of 5.4 Hz was used to eliminate resonance broadening due to the anisotropy of chemical shift tensors.

2.6. Conductivity measurements

Ionic conductivity measurements with alternating current were conducted on a AUTOLAB designed by Eco Chemie within the frequency range from 10 MHz to 10 Hz. The composite film was sandwiched between stainless steel blocking electrodes (1 cm diameter). The specimen thickness varied from 0.8 to 1.2 mm, and the impedance response was gauged over the range from 20 to 120 °C.

3. Results and discussion

3.1. XRD diffractional patterns

The PMMA/clay nanocomposite systems were synthesized via in situ intercalative polymerization using the Na^+-montmorillonite (MMT), which was organically modified by DDAC. The interlayer spacing of the PMMA/clay system was determined by the diffraction peak in the X-ray method, using the Bragg equation

$$\lambda = 2d \sin\theta$$

where d corresponds to the spacing between diffractional lattice planes; θ is the diffraction position and λ is the wavelength of the X-ray (1.5405 Å).

Fig. 2 shows the XRD patterns of the DDAC organically modified clay (Dclay) and various compositions of the PMMA/Dclay system in the range of diffractional angle $2\theta = 2-10°$. As would be expected, the well ion exchange between the clay (sodium cation) and the surfactant (ammonium cation) results in the increase of the basal interlayer spacing in comparison with the Na^+-MMT, and leads to a shift of the diffraction peak toward lower values of the θ. Furthermore, the polymer-intercalated behavior can also be confirmed by XRD pattern. From Table 1, the PMMA/Dclay binary blend at a low Dclay concentration (PMMA/Dclay = 100/2) has higher interlayer spacing (4.07 nm) than that of the Dclay (3.87 nm). Further increase

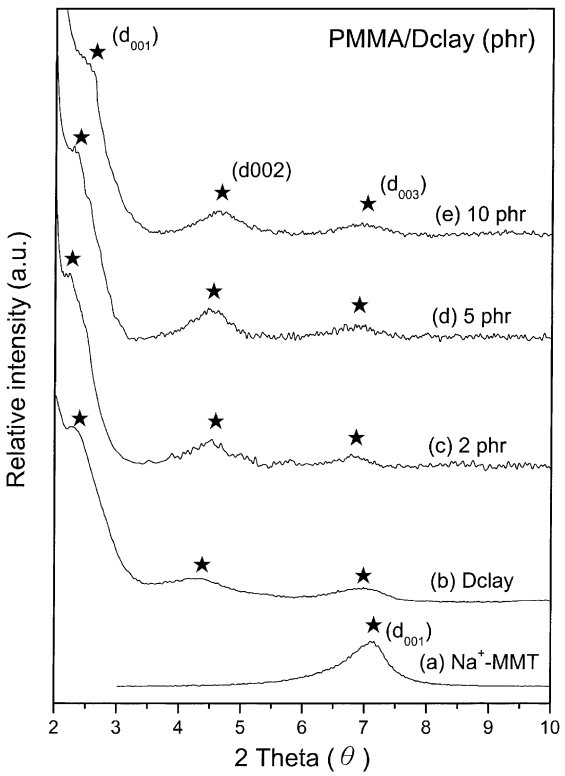

Fig. 2. XRD patterns of PMMA/Dclay hybrids containing various Dclay concentration (phr): (a) Na^+-MMT, (b) DDAC-MMT (Dclay), (c) 2 phr, (d) 5 phr, and (e) 10 phr.

Table 1
Basal spacing d_{001} (Å) after intercalated at various compositions

	DDAC-MMT	Composition PMMA/clay (phr)			
		2	5	8	10
Basal spacing (Å)	38.72	40.70	38.29	37.05	35.38

in the basal interlayer spacing implies that polymer chains are intercalated within the silicate galleries. The basal interlayer spacing decreases with the increase in the clay content due to less polymer chains intercalating within the galleries. Nevertheless, it is worth to point out that these PMMA/clay blends are nanosized composites (3–4 nm) exhibiting marked surface area of these silicate layers.

3.2. Infrared spectra

Since the carbonyl group (C=O) is a strong electron donor within the PMMA-based polymer electrolyte, the Li^+ ion tends to complex with the oxygen atom of the carbonyl group. Infrared is a powerful tool to monitor such ionic interaction. According to previous publications [22–24], the peak at 1729 cm^{-1} in Fig. 3 represents the free C=O group of the PMMA. When the specific amount of the $LiClO_4$ salt (mole ratio C=O/Li^+ = 8) is added, a weak shoulder at 1700 cm^{-1} appears corresponding to the interaction between the lithium cation and the C=O group. The relative intensity of the shoulder at 1700 cm^{-1} increases with increasing the Dclay content without any chemical shift. This observation indicates that the presence of the Dclay is able to enhance the interaction between the PMMA carbonyl and the lithium cation.

The $\nu(ClO_4^-)$ internal mode of the $LiClO_4$ displays a similar trend. The $\nu(ClO_4^-)$ internal mode is particularly sensitive to the local anionic environment [25–28]. According to prior literature [25,28], the component

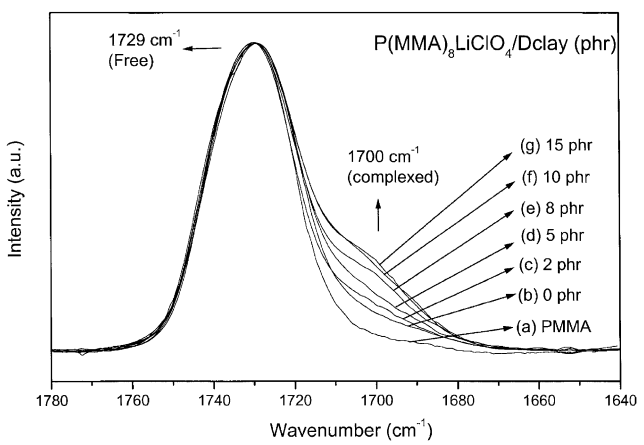

Fig. 3. Infrared spectra of the carbonyl-stretching mode (C=O group) for $P(MMA)_8LiClO_4$/Dclay composite electrolytes with various Dclay concentration (phr): (a) PMMA, (b) 0 phr, (c) 2 phr, (d) 5 phr, (e) 8 phr, (f) 10 phr, and (g) 15 phr.

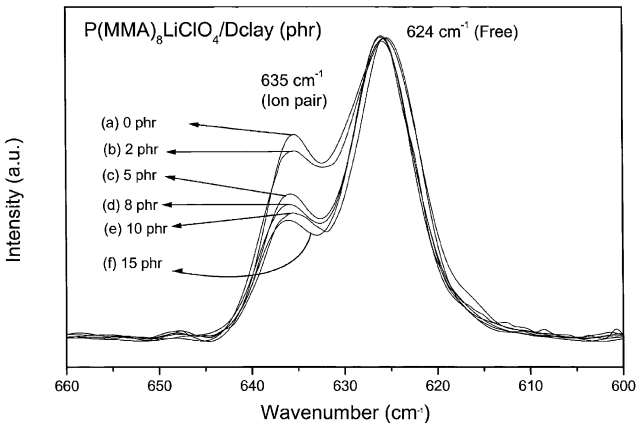

Fig. 4. Infrared spectra of $\nu(ClO_4^-)$ internal modes for $P(MMA)_8LiClO_4$/-Dclay composite electrolytes with various Dclay concentration (phr): (a) 0 phr, (b) 2 phr, (c) 5 phr, (d) 8 phr, (e) 10 phr, and (f) 15 phr.

observed at ~624 cm^{-1} has been assigned to the free anion which does not interact directly with the lithium cation. Component at ~635 cm^{-1} has been attributed to the contact ion pair. Fig. 4 presents typical infrared spectra of the $\nu(ClO_4^-)$ spectral ranging from 660 to 600 cm^{-1} recorded at 120 °C for $P(MMA)_8LiClO_4$/Dclay ternary blends with different Dclay concentrations. As shown in Fig. 4, the weak peak of the ion pair (~635 cm^{-1}) decreases gradually with increasing Dclay content, an indication of higher dissociability of the lithium salt. In order to further clarify the effect of Dclay on the charge environment surrounding the carbonyl group of the PMMA and the lithium anion of $LiClO_4$, relative fraction of the 'complexed' C=O site and the free anion have been quantified by decomposing the C=O stretching band and the $\nu(ClO_4^-)$ internal mode into two Gaussian peaks. Table 2 and Fig. 5 summarize relative fractional area and locations of related adsorption bands for comparison. As shown in Fig. 5, both relative fraction of the complexed C=O sites and the free anions increase with increasing Dclay content. In other words, the formation of

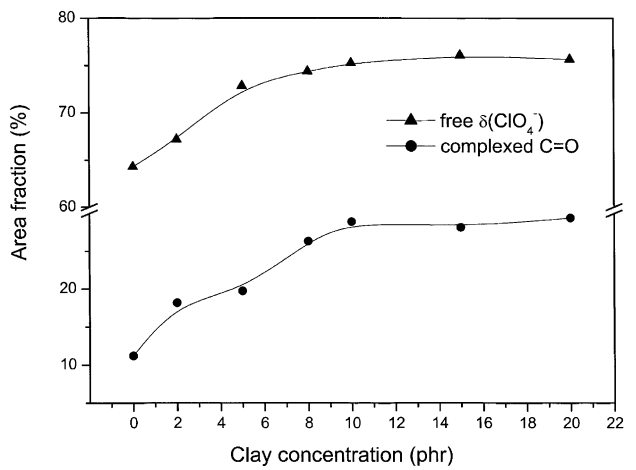

Fig. 5. Fraction of free $\nu(ClO_4^-)$ internal mode and complexed C=O site versus Dclay concentration for $P(MMA)_8LiClO_4$/Dclay composite electrolytes at 125 °C: (▲) free $\nu(ClO_4^-)$, (●) complexed C=O site.

Table 2
Curve-fitting data of infrared spectra of C=O stretching region and $\nu(ClO_4^-)$ internal mode of $P(MMA)_8LiClO_4$/clay complexes with various clay concentrations at 120 °C

Clay concentration (phr)	Complexed C=O		Free anion	
	ν (cm^{-1})	A_c (%)	ν (cm^{-1})	A_f (%)
0		11.21	625.9	64.27
3	1730.4	18.19	625.6	67.19
5	1730.9	19.75	625.9	72.85
8	1731.1	26.34	625.9	74.39
10	1731.2	28.91	625.6	75.25
15	1730.4	28.17	626.0	76.09
20	1730.8	29.42	625.9	75.66

the complexed C=O sites accompanies with higher fraction of the free anions. The addition of the Dclay mineral tends to attract the carbonyl group (C=O) to interact with the lithium salt ($LiClO_4$). This phenomenon can also be related to the dipoles within the clay mineral. According to our prior studies [19,20], clay is a natural mineral with high dielectric constant. If the clay layers are well dispersed in the polymer matrix, dielectric property of the system increases. In order to further interpret this interacting mechanism, the well-dispersed clay layers in the PMMA based polymer electrolyte system are illustrated in Fig. 6. Fig. 6 shows that each silicate layer possesses numerous negative charges, and great numbers of the well-dispersed clay layers can produce huge numbers of dipoles. Therefore, the charge environment in the system is greatly disturbed

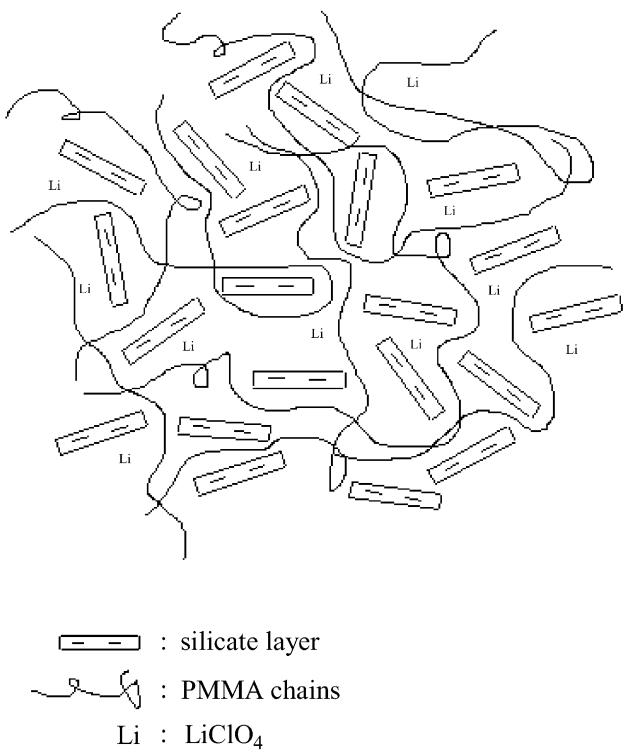

Fig. 6. Schematic structure of the complex formed by Li^+ cation, PMMA chains and silicate layers.

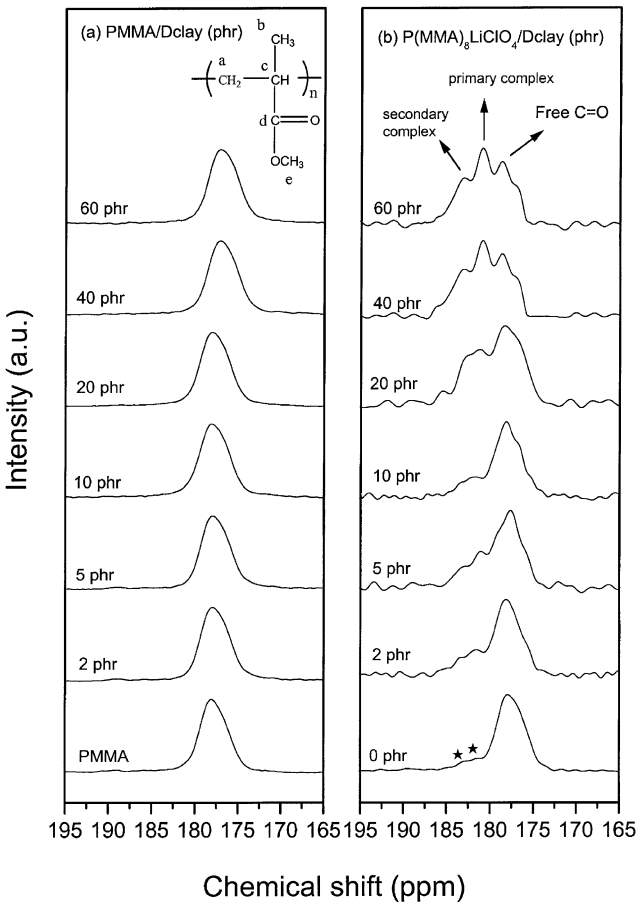

Fig. 7. Scaled ^{13}C CP/MAS NMR spectra region ranging from 195 to 165 ppm for PMMA-based composite with various Dclay content: (a) PMMA/Dclay (b) $P(MMA)_8LiClO_4$/Dclay.

and provides a good environment to dissolve the lithium salt. As a result, the lithium salt be dissolved more easily, and the carbonyl group (C=O) in the PMMA can have more chances to interact with the free lithium cation.

3.3. Solid-state NMR

The solid-state NMR spectrum is used to characterize the interaction behavior between PMMA, lithium salt and Dclay mineral. The electron-donated carbon produces a small perturbation to the magnetic shield on the nucleus and results in downfield chemical shift as compared to the ones without the complex interaction [29,30]. On the contrary, the electron-accepted carbon tends to shift upfield. Fig. 7 shows the scale expanded ^{13}C CP/MAS NMR spectra containing various Dclay concentrations to present the peak assignments for $P(MMA)_8LiClO_4$/Dclay ternary blends and the corresponding PMMA/Dclay binary blends. The resonance of the carbonyl carbon of the PMMA (C_d) is assigned at 178.0 ppm. As shown in Fig. 7(a), no apparent chemical shift can be observed, indicating that the interaction between the silicate layer and the C=O is insignificant. When the $LiClO_4$ is incorporated into the system as shown in Fig. 7(b), two minor shoulders appear at 181.4 and 182.8 ppm. It is reasonable to assign that the shoulder at 181.4 ppm is the primary complex of $Li^+\cdots C{=}O$ and the shoulder at 182.8 ppm is the secondary complex between Li^+ and several C=O groups simultaneously [1,31,32]. When the Dclay is added incrementally, both shoulders increase gradually and eventually become two new bands. The relative intensity of the new band at 181.4 ppm, representing the primary complex, increases more rapidly than that of the 182.8 ppm band with increasing Dclay concentration, and eventually becomes dominant when the Dclay concentration is greater than 40 phr. The basicity of the C=O group in PMMA is increased with the increase in the Dclay content, implying that the C=O group is able to act as a strong electron donor to interact with the Li^+ ion. This observed phenomenon is consistent with the infrared result. The strong interaction between the C=O group and the Li^+ come from the dipoles within the silicate layers that facilitate the dissolution of the lithium salt.

The identical trend can also be observed in the C_b resonance (Fig. 8). The resonance of the C_b is assigned at 52.3 ppm. Similar to that of the C_d resonance, no chemical shift can be found in these PMMA/Dclay binary blends, indicating that the electron surrounding the C_b atom is not affected by the Dclay. Nevertheless, the chemical shifts of the C_b can be found when the lithium salt is added. In the ternary blend of the $P(MMA)_8LiClO_4$/Dclay, the C_b band

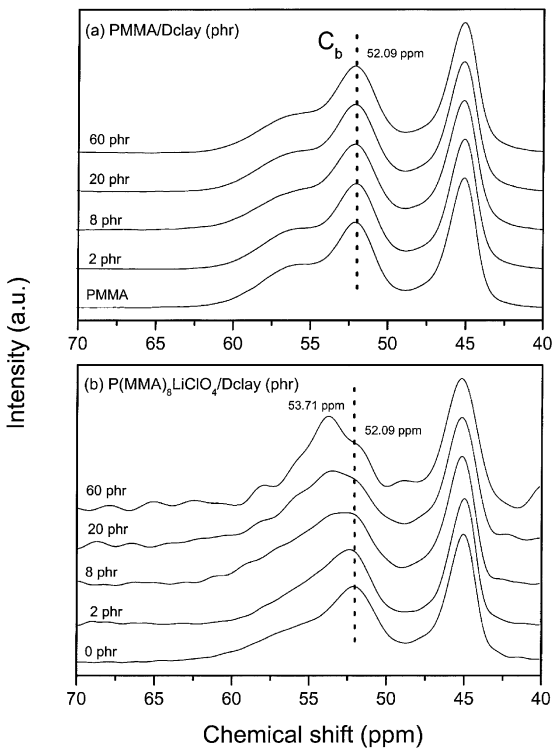

Fig. 8. Scaled ^{13}C CP/MAS NMR spectra region ranging from 70 to 40 ppm for PMMA-based composite with various Dclay content (phr): (a) PMMA/Dclay, (b) $P(MMA)_8LiClO_4$/Dclay.

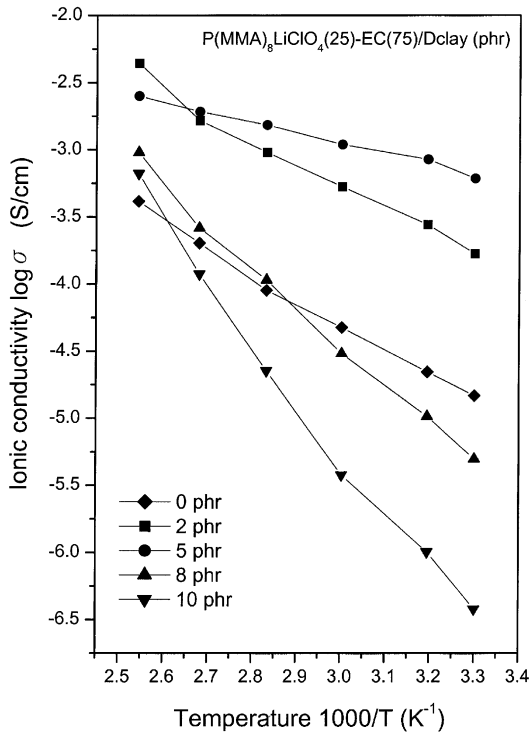

Fig. 9. Arrhenius conductivity plots for $P(MMA)_8LiClO_4$(25)-EC(75)/Dclay composite electrolyte containing various Dclay content (phr): (◆) 0 phr, (■) 2 phr, (●) 5 phr, (▲) 8 phr, and (▼) 10 phr.

shifts to the higher ppm progressively with the increase in the Dclay content. The chemical shifting toward higher ppm indicates that its surrounding electrons have been deprived by the higher electronegativity of the C=O. It is reasonable to assume that the withdrawing group (C=O) is partially compensated by drawing electrons from the neighboring C atoms, and results in a slight positive charge on these neighboring C atoms [33,34]. This observation indicates that the strong interaction between C=O and Li^+ occurs when the Dclay is added.

3.4. Conductivity

In order to achieve the commercial purpose, the study on the effect of adding specific amount of EC to the $P(MMA)_8LiClO_4$/Dclay system has been carried out. Fig. 9 presents the Arrhenius plots illustrating the temperature dependence on the ionic conductivity of the $P(MMA)_8LiClO_4$(25)/EC(75)/Dclay electrolyte nanocomposites containing various Dclay concentrations. The conductivity increases with the increase in the Dclay content and attains a maximum value when the Dclay concentration is at 5 phr. Subsequently, the conductivity decreases drastically with further increase in the Dclay content. Fig. 10 plots the conductivity versus Dclay content for the $P(MMA)_8LiClO_4$(25)/EC(75)/Dclay composite electrolytes at 30 °C. A rapid increase in the conductivity is observed by adding small quantity of the Dclay and the maximum ionic conductivity is achieved at 5 phr Dclay concentration.

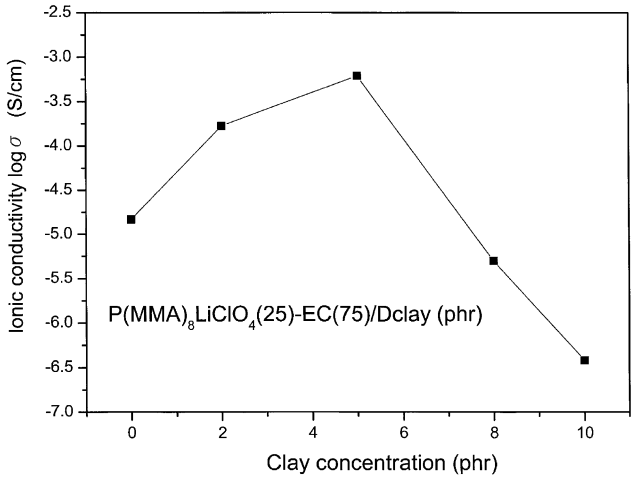

Fig. 10. Ionic conductivity versus Dclay content for $P(MMA)_8LiClO_4$(25)-EC(75)/Dclay composite electrolyte at 30 °C.

When the Dclay is increased to 8 phr or higher, the conductivity decreases even lower than the original value. The conductivity behavior can be interpreted by the following equation

$$\sigma = \sum_i n_i z_i \mu_i$$

where n_i, z_i, and μ_i refer to the number of the charge carrier, ionic charge and the ionic mobility. According to the above equation, the ionic conductivity depends on the amount of charge carriers (n_i) in the system and the mobility (μ_i) of the various species. From the FTIR and NMR results, the addition of the Dclay is able to increase fraction of the free anion and results in higher charge carrier (n_i). However, the addition of the clay mineral also results in lower chain mobility (due to the increase in the viscosity) and thus decreases the ionic mobility (μ_i). These two adverse and competitive effects occur in this system, one is favorable and other is unfavorable for the ionic conductivity. It can be concluded that the addition of an optimum Dclay content (5 phr) provides the most suitable environment for the ionic transportation and achieves the highest conductivity. Notably, the highest conductivity (6×10^{-4} S cm^{-1}) is achieved with 5 phr Dclay in the $P(MMA)_8LiClO_4$/EC system, which is nearly 40 times higher than the original $P(MMA)_8LiClO_4$/EC system.

In order to further clarify this assumption, the plasticizer effect on the ionic conductivity is illustrated in Fig. 11. The conductivity of the plain electrolyte system (without clay) increases progressively with EC content and approaches a plateau at about 60%. This conductivity behavior is consistent with the general observation of polymer salt electrolytes. This phenomenon can be attributed to the increase in chain mobility due to the reduction of system's viscosity at a higher EC concentration. Meanwhile, the increase in the EC content will decrease the lithium salt concentration and thus lowers the number of the charge

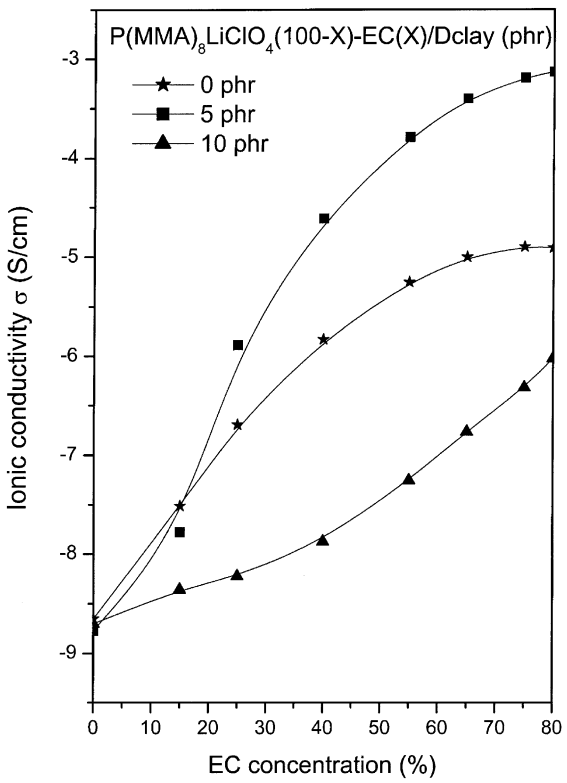

Fig. 11. Ionic conductivity versus EC content for $P(MMA)_8LiClO_4(100-X)$-EC(X)/Dclay composite electrolyte containing various Dclay content (phr) at 30 °C: (★) 0 phr, (■) 5 phr, and (▲) 10 phr.

carrier (n_i). It appears that the inclusion of the EC (increase μ_i) dominates the concentration effect (lower n_i) and results in higher conductivity. A similar trend is observed with the addition of the clay mineral except that the conductivity increase is more significant. Nevertheless, an opposed trend is observed when the Dclay is at 10 phr, the conductivity also increases with the increase in the EC content but its extent is significantly lower than that of the plain electrolyte system. The inclusion of the clay mineral possesses two adverse and competitive effects on the resultant conductivity in this system. The higher clay content results in higher dissociation of the lithium salts favorable for higher conductivity and higher viscosity unfavorable for conductivity. These novel plasticized nanocomposite films not only give significantly higher conductivity but also possess improved dimensional stability for potential commercial applications.

4. Conclusion

This study has demonstrated that the addition of an optimum content of the organo-modified montmorillonite increases the ionic conductivity of the PMMA-based electrolyte by nearly 40 times relative to the plain $P(MMA)_8LiClO_4(25)$/EC(75) system. X-ray characterization indicates that the polymer chains are intercalated within silicate gallery and expand the surface area of silicate layers significantly. FTIR and solid-state NMR studies have demonstrated that specific interactions exist among the PMMA, clay mineral and $LiClO_4$. FTIR results indicate that both relative fractions of the complexed C=O and the free anion increase with the addition of the Dclay. The presence of the Dclay is able to facilitate the C=O group to interact with the lithium salt. NMR results show insignificant interaction between the Dclay and the PMMA. The addition of well-dispersed silicate layers can facilitate the dissociation of the lithium salt and results in more fraction of free lithium cation to interact with the C=O group. However, a balanced and optimum attractive forces among silicate layers, C=O groups and lithium cation results in the highest ionic conductivity.

References

[1] Scrosati B. In: MacCallum JR, Vincent CA, editors. Polymer electrolyte reviews. New York: Elsevier; 1989. p. 315.
[2] Scrosati B. In: Scrosati B, editor. Applications of electroactive polymers. New York: Chapman & Hall; 1993. p. 251.
[3] Armand MB. Solid State Ionics 1983;9–10:745.
[4] Chao S, Wrighton MS. J Am Chem Soc 1987;109:2197.
[5] Armand MB. Annu Rev Mater Sci 1986;16:245.
[6] Ratner MA, Shriver DF. Chem Rev 1988;88:109.
[7] Armand MB, Sanchez JY, Gauthier M, Choquette Y. In: Liplowski J, Ross PN, editors. Polymeric materials for lithium batteries, in the electrochemistry of novel materials. New York: VCH; 1994. p. 65.
[8] Scrosati B, Neat RJ. In: Scrosati B, editor. Applications of electroactive polymers. London: Chapman & Hall; 1993. p. 182.
[9] Chu PP, He ZP. Polymer 2001;42:4743.
[10] Kim HT, Kim KB, Kim SW, Park JK. Electrochim Acta 2000;45:4001.
[11] Song JY, Wang YY, Wan CC. J Power Sources 1999;77:183.
[12] Labrèche C, Lévesque I, Prud'homme J. Macromolecules 1996;29:795.
[13] Rajendran S, Uma T. Mater Lett 2000;44:242.
[14] Rajendran S, Kannan R, Mahendran O. Mater Lett 2001;49:172.
[15] Stephan AM, Renganathan NG, Kumar TP, Thirunakaran R, Pitchumani, Shrisudersan J, Muniyandi N. Solid State Ionics 2000;130:123.
[16] Feuillade G, Perche Ph. J Appl Electrochem 1975;5:63.
[17] Bohnke O, Frand G, Rezrazi M, Rousselot C, Truche C. Solid State Ionics 1993;55:105.
[18] Appetecchi GB, Crose F, Scrosati B. Electrochim Acta 1995;40:991.
[19] Chen HW, Chang FC. Polymer 2001;42:9763.
[20] Chen HW, Chang FC. J Polym Sci, Part B: Polym Phys 2001;39:2407.
[21] Ogata N, Kawakage S, Ogihara T. Polymer 1997;38:5115.
[22] Kuo SW, Lin CL, Chang FC. Macromolecules 2002;35:278.
[23] Li D, Brisson J. Polymer 1998;39:793.
[24] Li D, Brisson J. Polymer 1998;39:801.
[25] Mishra R, Rao KJ. Solid State Ionics 1998;106:113.
[26] Xuan X, Wang J, Tang J, Qu G, Lu J. Spectrochim Acta, Part A 2000;56:2131.
[27] Wang Z, Huang B, Huang H, Chen L, Xue R. Solid State Ionics 1996;85:143.
[28] Salomon M, Xu M, Eyring EM, Petrucci S. J Phys Chem 1994;98:8234.
[29] Wu HD, Ma CCM, Chang FC. Macromolecules 1999;32:3097.

[30] March T. In: March T, editor. Advanced organic chemistry—reactions, mechanism, and structure, 3rd ed. New York: Wiley; 1985. p. 14.
[31] Lee JY, Painter PC, Coleman MM. Macromolecules 1988;21:954.
[32] Gray FM. Polymer electrolytes. Cambridge, UK: Royal Society of Chemistry; 1997.
[33] Williamson. J Am Chem Soc 1963;85:516.
[34] Laszol, Schkeyer J. J Am Chem Soc 1963;85:2709.